



Earthquake Hazards Team

Sensitivity of Earthquake Loss Estimates to Source Modeling Assumptions and Uncertainty

By Paul A. Reasenber, Nan Shostak, and Sharon Terwilliger

Open-File Report 2006-1020

**U.S. Department of the Interior
U.S. Geological Survey**

U.S. Department of the Interior

Gale A. Norton, Secretary

U.S. Geological Survey

P. Patrick Leahy, Acting Director

U.S. Geological Survey, Reston, Virginia 2006

Revised and reprinted: 2006

For product and ordering information:

World Wide Web: <http://www.usgs.gov/pubprod>

Telephone: 1-888-ASK-USGS

For more information on the USGS—the Federal source for science about the Earth, its natural and living resources, natural hazards, and the environment:

World Wide Web: <http://www.usgs.gov>

Telephone: 1-888-ASK-USGS

Any use of trade, product, or firm names is for descriptive purposes only and does not imply endorsement by the U.S. Government.

Although this report is in the public domain, permission must be secured from the individual copyright owners to reproduce any copyrighted material contained within this report.

Introduction

This report explores how uncertainty in an earthquake source model may affect estimates of earthquake economic loss. Specifically, it focuses on the earthquake source model for the San Francisco Bay region (SFBR) created by the Working Group on California Earthquake Probabilities (WGCEP, 2003). The loss calculations are made using HAZUS-MH (2003), a publicly available computer program developed by the Federal Emergency Management Agency (FEMA) for calculating future losses from earthquakes, floods and hurricanes within the United States. The data base built into HAZUS-MH includes a detailed building inventory, population data, data on transportation corridors, bridges, utility lifelines, etc. Earthquake hazard in the loss calculations is based upon expected (median value) ground motion maps called ShakeMaps (Wald et al., 1999) calculated for the scenario earthquake sources defined in WGCEP (2003)¹.

The study considers the effect of relaxing certain assumptions in the WG02 model, and explores the effect of hypothetical reductions in epistemic uncertainty in parts of the model. For example, it addresses questions such as What would happen to the calculated loss distribution if the uncertainty in slip rate in the WG02 model were reduced (say, by obtaining additional geologic data)? What would happen if the geometry or amount of aseismic slip (creep) on the region's faults were better known? And what would be the effect on the calculated loss distribution if the time-dependent earthquake probability were better constrained, either by eliminating certain probability models or by better constraining the inherent randomness in earthquake recurrence?

The study does not consider the effect of reducing uncertainty in the hazard introduced through models of attenuation and local site characteristics, although these may have a comparable or greater effect than does source-related uncertainty (Grossi, 2000; Cao and Petersen, in press). Nor does it consider sources of uncertainty in the building inventory, building fragility curves, and other assumptions adopted in the loss calculations. This is a sensitivity study aimed at future regional earthquake source modelers, so that they may be informed of the effects on loss introduced by modeling assumptions and epistemic uncertainty in the WG02 earthquake source model.

Theoretical background

A fully probabilistic formulation for loss is presented in Cao et al. (1999). Their approach involves conditional probability density functions that represent the dependence of MMI on peak ground motions and the dependence of loss on MMI. Cao et al's (1999) probabilistic expression for loss is

$$f_L(l) = \int di \int f_L(l|i) f_I(i|a) f_A(a) da \quad 1$$

where $f_L(l)$ is the pdf for loss; $f_I(l|i)$ is the conditional pdf for loss, given MMI; $f_I(i|a)$ is the conditional pdf for MMI, given acceleration; and $f_A(a)$ is the pdf for acceleration.

We replace $f_I(i|a)$ with a deterministic relationship between PGA and MMI (Wald et al., 1999) (Table 1, Figure 1) defined for nine values of MMI.

¹ The WGCEP (2003) study was substantially completed in 2002 and is commonly referred to as "WG02". Hereafter we shall refer to this study as WG02.

Table 1. ShakeMap Instrumental Intensity as a function of PGA (Wald et al., 1999)

PGA (g)	MMI
0.001	1
0.00785	2.5
0.0265	4
0.0655	5
0.136	6
0.26	7
0.495	8
0.945	9
1.24	10

We replace $f_L(l|i)$ with a deterministic relationship between MMI and a measure of the fractional loss of built structures derived from a survey of expert opinion (ATC-13, their Table 7.10) (Table 2, Figure 2). ATC-13 provides the probability of exceeding certain damage levels, given the MMI level and building class. From these, we derive the mean damage in wood frame buildings, given MMI.

Table 2. ATC-13 Mean Central Damage Factor¹ as a function of MMI.

MMI	Mean Central Damage Factor (%)
6	1.73
7	3.79
8	5.45
9	10.6
10	21.4
11	25.5
12	39.4

1. ATC-13 defines Central Damage Factor as the ratio of the dollar loss to replacement value of a structure.

Next, we construct continuous functions for the conditional pdf's

$$f_{Wald}(i|a) = c_1 a^{c_2} - c_3 \quad 2a$$

$$f_{ATC}(l|i) = c_4 e^{c_5 i} - c_6 \quad 2b.$$

The constants $c_1 - c_6$ are chosen so that these functions approximate the respective tabulated values from Wald et al. (1999) and ATC-13. In Equation 2a, $c_1 = 12.7$, $c_2 = 0.15$, $c_3 = 3.4$, intensity is in MMI units and acceleration is in g. In Equation 2b, $c_4 = 0.4$, $c_5 = 0.4$, $c_6 = 3.0$, intensity is in MMI units and loss is expressed as the Central Damage Factor (CDF).

Adopting the deterministic relationships in Equation (2) simplifies the calculation of $f_L(l)$ in Equation (1). Lee (1960) provides a method for calculating the probability density function for a random variable $y = f(x)$, given the probability density function for x . If $P_y(y)$ and $P_x(x)$ are the pdf's for the random variables y and x respectively, then

$$P_y(y) = \frac{P_x(x)}{|f'(x)|} \Bigg|_{x=g(y)} \quad 3$$

where $f'(x)$ denotes $\frac{dy}{dx}$ and $x = g(y)$ is the inverse of $y = f(x)$. Equation (3) requires that f have an inverse. For the relationships in Equation (2) between acceleration and MMI, and between MMI and loss, this requirement is met. The transformation of pdf in Equation (3) is applied twice, first to the pdf for acceleration to get the pdf for MMI, and then to the pdf for MMI to get the pdf for loss.

Analytical Example

To illustrate these transformations, we consider the probability density function for acceleration at a single site associated with a single earthquake source. We use three truncated Gaussians (with constant mean=0.5g and varying variance) to represent possible pdf's for PGA (Figure 2). First, we transform these into pdf's for MMI, using Equation 2a (Figure 3). This transformation introduces an increase in median MMI with increasing variance in acceleration. This effect arises from the non-linear dependence of MMI on PGA, with MMI dropping steeply with decreasing values of PGA below 0.5g.

Next we transform the pdf's for MMI into ones for Central Damage Factor (CDF), using Equation 2b (Figure 4). (ATC-13 defines central damage factor for a structure as the actual economic loss sustained divided by total replacement value of the structure, i.e., the fractional loss.) Here, we see the accumulated effect of the Wald and ATC-13 transformations on the loss distribution. The probability distribution for loss skews to the right with increasing standard deviation in acceleration (still, for a fixed mean PGA of 0.5). The skew is the result of two factors. First, the exponential shape of the ATC-13 transformation from MMI to CDF (Figure 1b) extends the upper tail for CDF. At the same time, damage drops to zero for MMI levels of approximately 5 and less, so there is little contribution to damage from the lower levels of MMI. The fattened left tail in the distribution for MMI contributes virtually nothing to the likelihood for damage. The combined effect of the Wald and ATC-13 transformation is to skew the loss distribution to the right (and to greatly extend the right tail, or "worst-case" loss) with increasing variance in the hazard. The mean CDF for the distributions in Figure 4 are 7.0, 7.5 and 9.0 (standard deviation in PGA of 0.05, 0.2 and 0.4, respectively), while the 95%-ile values of CDF are 9.2, 13.6 and 18.1, respectively. From the probability density functions for loss, loss exceedance (LE) curves are easily constructed (Figure 5).

Figure 5 illustrates the main point of this exercise. We see in the transformations from PGA to loss in the foregoing examples that symmetrically increasing uncertainty in hazard skews the loss distribution to the right and substantially increases worst-case (5% or 1% exceedance probability) loss estimates. For economic models sensitive to the worst-case loss such as ones in the insurance industry, reducing epistemic uncertainty in hazard, keeping all other factors unchanged, can have significant impact by substantially lower the estimated worst-case loss.

Another contribution to the right-shift in the loss exceedance curves in this particular example (Figure 5) comes from the fact that the distribution for PGA (Figure 2) is truncated at zero for the larger variance distributions (standard deviations in acceleration of 0.2 g and 0.4 g), slightly violating the assumption of symmetric variance in acceleration. However, this artifact contributes only slightly to the total shift in probability in Figure 5, and was ignored in this exercise.

Earthquake loss estimates and the WG02 source model

In this section we explore the economic earthquake-related losses in Alameda County, California. Limiting the calculations to Alameda County was done for expediency: a HAZUS-MH (2003) calculation of direct economic loss for Alameda Co. takes approximately 30 minutes on a 3.2 gigahertz PC with 2 gigabytes of memory; the corresponding calculation for the 10-county SFBR takes 5 times as long, and approximately 250 runs were needed. While confining the calculations to Alameda Co. emphasizes the uncertainties associated with the Hayward and Calaveras faults, relative to those for the other major faults in the SFBR, we do not believe that this provinciality significantly affects the overall results of the study. To calculate the losses, we follow and build upon a methodology pioneered by Grossi (2000). Grossi (2000) estimated the direct economic losses to homeowners and the insurance industry in the Oakland, California, region and explored the sensitivity of these losses to uncertainties in the recurrence rates of earthquakes,

attenuation models for ground motion, soil mapping schemes, and exposure vulnerability and loss parameters, using the HAZUS-MH software (HAZUS, 2003). In addition, Grossi (2000) explored the benefits and costs of structural mitigation to wood frame residential structures in the Oakland region. Grossi (2000) used 32 discrete earthquake sources, their annual recurrence rates, and soils and attenuation models provided in HAZUS. The latter include the empirical relationships of Boore et al. (1993, 1994); Sadigh et al. (1993); and Campbell and Bozorgenia (1994).

While other earthquake loss estimation programs exist and are used by private companies that model earthquake risk, they are all (to our knowledge) proprietary. HAZUS-MH was chosen for this study because it is publically available.

In this study, we explore distributions of economic loss in all of Alameda County, California. The loss calculations are based on the 42 earthquake rupture sources in the WG02 earthquake model for the San Francisco Bay region. Ground motion hazard maps are calculated for each of these sources using the OpenSHA software “ScenarioShakeMapApp.jar” (Field et al., 2003, 2005). These ground motion hazard maps are the input for HAZUS-MH, which is used to estimate the direct economic loss in Alameda County for each scenario earthquake source. In the loss calculations, we use the default building inventory, exposure and damage calculations built into HAZUS-MH.

The WG02 model is a Monte Carlo simulation consisting of, in this study, typically 3000 iterations. Each iteration produces an estimate of the long-term mean magnitude and long-term mean annual rate of recurrence for each earthquake source. Thus, each run of the WG02 code produces a distribution of mean magnitude and mean annual rate for each rupture source. We convolve these distributions with the results of loss calculations to obtain annualized loss exceedance (LE) curves reflecting all of the uncertainty in the WG02 model. The LE curve is analogous to the hazard curve. The latter shows the frequency of exceeding a given level of ground motion at a specified site in a specified time interval. The LE curve shows the frequency of exceeding a given level of annualized economic loss in a specified area for a specified class of structures. These LE curves are then used to support a number of risk de-aggregation and sensitivity studies, which are the topic of the next section of this report. In this study, uncertainty in attenuation relation and site response are not represented. In the remainder of the present section, we define terms and describe in some detail the calculations leading to loss exceedance curves.

Loss exceedance curves are constructed for a given region, building inventory, set of attenuation relations and site amplification factors, and a probabilistic earthquake source model. The following terms, used below to describe the loss calculations, are defined here.

1. *Region*. In the most general application of this method, the region consists of a set of discrete areas (e.g., counties) in the SFBR, denoted by subscript k . In the present study, there is only one region: Alameda County ($k=1$).
2. *Rupture source*. Any of the 42 rupture sources defined in WG02. These include 35 fixed-segment sources (e.g., RC, HN, HN+HS, etc.) and 7 “floating sources.” Rupture sources are denoted by subscript j .
3. *Rupture mean magnitude*. In each Monte Carlo iteration in the WG02 calculation, a mean magnitude is associated with each rupture source.
4. *Assumptions*. Any particular set of assumptions and model constraints used in the WG02 model is denoted by subscript i . The assumptions and constraints may relate to source specification (e.g., constrain the rupture source depths, constrain the uncertainty in fault slip rates, use only a subset of the faults in the region); probability model (e.g., use only the Poisson probability model); or any other set of constraints on the calculation (e.g., use a single M-log A relation, consider only sources with magnitudes in a specified range, increase or decrease the amount of aseismic slip on faults, etc.).
5. An *iteration* in a Monte Carlo run of WG02 is denoted by subscript q . Each iteration produces a complete description of one possible realization of the WG02 model. Typically, 3000 iterations were used in this study. It is the iteration over q that produces the distribution in loss.

In each iteration, the following are calculated for each rupture source: rupture geometry; mean magnitude; long-term annual rate of rupture; and (time-dependent) probability of rupture (in T years). These are, respectively,

$$G_j^q, m_j^q, \lambda_j^q, P_j^q(T) .$$

Mean magnitude

In the WG02 model, the mean magnitude of an earthquake is determined by the area of the rupture source that produced it, which is to say, by the length and width of the rupture source, with a possible adjustment for a specified amount of aseismic slip. And since the rupture sources are defined by fault segments whose endpoints and seismogenic thickness are uncertain, the area (and, hence, magnitude) of earthquakes from a given rupture source are distributed over some range.

Rupture geometry

The length of fault and width of the seismogenic slip vary in each iteration, and the effect of this variance on the loss calculation is carried through the mean magnitude, as just noted. We do not, however, directly consider variations in rupture geometry when calculating the ground motions. Instead, we always use the mean geometry in calculating ground motions for each rupture source (even though the magnitudes vary). Thus, all variance in the source associated with epistemic uncertainty in rupture geometry is conveyed to the ground motion calculations through the mean magnitude. This simplification omits variance associated with the specific endpoints and width of the rupture. Such variations should be significant in hazard calculations only very close to the rupture source endpoints.

Annual rate of rupture

For each iteration in the WG02 Monte Carlo calculation, the long-term annual rupture rate is calculated for each rupture source. The mean annual rate is used in calculating the annual loss associated with each rupture source.

Probability of rupture in T years.

Uncertainty associated with the use of time-dependent probability models in the WG02 model can be captured by substituting for the mean annual rate an effective Poisson rate λ_{Pois}^{td} that corresponds to the (time-dependent) probability, P_{td} , of rupture in T years.

$$\lambda_{Pois}^{td} = \frac{-1}{T} \ln(1 - P_{td}).$$

Scenario earthquake sources

For each of the WG02 rupture sources, we calculate ground motion hazard maps for a set of earthquake magnitudes. The magnitude set spans the range of mean magnitude for the rupture source determined by the WG02 model, with 0.1 magnitude unit spacing. For example, we calculate ground motion maps for rupture source “SAS+SAP” at magnitudes $\hat{m}=7.1, 7.2, 7.3, 7.4, 7.5,$ and 7.6 , since the mean magnitude for this rupture in the Monte Carlo iterations is in the range (7.1—7.6). This procedure allows us to capture uncertainty in hazard associated with the source magnitude. When all rupture sources and their respective ranges of magnitude are considered, we find that we must calculate 250 separate sets of ground motion maps.

Ground motion calculations.

For each rupture source, we calculate site-dependent ground motions using the OpenSHA software “ScenarioShakeMapApp.jar” (Field et al., 2003; Field et al., 2005b) We first calculate maps of peak acceleration, peak velocity and spectral acceleration at 0.3 s and 1.0 s period, on rock-sites, exactly as in the 2002 National Hazard Maps for the western U.S. (Frankel et al., 2002). These are then multiplied by Borchardt’s (1994) non-linear amplification factors, to get the site-dependent hazard maps.

HAZUS-MH calculations

The first step toward calculating the distribution of loss in region k implied by the WG02 model with Assumptions A_i is to calculate the loss $L_{i,j,k}$ associated with each rupture source-magnitude combination $(G_j, \hat{m}_j), j=1, 41$. This requires running Hazus-MH 250 times for each region.

Next, we sum (over all sources) the product of the loss in region k associated with source j and the mean annual rate of occurrence of source j to get the mean annual loss (MAL) in region k for Monte Carlo iteration q ($q=1, N$):

$$MAL_{i,k}^q = \sum_{j=1}^{41} \lambda_j^q L_{i,j,k}(G_j, \hat{m}_j^q)$$

Finally, we look at the distribution of $MAL_{i,k}^q$ for certain sets of assumptions A_i . We calculate mean annual loss exceedance curves for Alameda County, using the Hazus-MH “Total Direct Economic Loss” (DEL) calculations. DEL includes the economic losses associated with all types of buildings in the HAZUS-MH inventory coming from building damage, contents damage, inventory loss, relocation costs, income loss, rental income loss and wages loss. Direct economic loss does *not* include losses due to interruption of business, increased social services, reduced tax revenues, etc., that also would result from a major quake.

The Monte Carlo calculation produces N realizations (typically, $N=3000$). The best estimate of the true MAL for the region is the median of this distribution. A confidence interval for this estimate of MAL is obtained from the distribution in the usual way. MAL is synonymous with “annual risk”.

Scenario earthquake ruptures: Ground motions and economic loss in Alameda County

In this section we look at four particular scenario earthquakes considered by WG02. Over the long term, these four scenario earthquakes are the four greatest contributors to Alameda County’s earthquake risk (Figure 6b). The rupture sources in these scenarios – a rupture of the southern Hayward fault (HS); a rupture of the entire Hayward fault (HS+HN); a rupture of the northern Calaveras fault (CN); and a rupture of the San Andreas fault from the Santa Cruz mountains to Cape Mendocino (SAS+SAP+SAN+SAO) – are defined in WG02. The earthquake magnitudes in the four scenarios are the respective mean magnitudes calculated in WG02.

Losses for these scenarios are calculated with HAZUS-MH. Site-dependent ground motions used in the HAZUS-MH calculations (PGA, PGV, and spectral acceleration at 0.3 and 1.0 sec period) were calculated for rock sites using the OpenSHA software “ScenarioShakeMapApp.jar” (Field et al.), exactly as in the 2002 National Hazard Maps for the western U.S. (Frankel et al., 2002). For each scenario we show (Figures A1 – A4) only the spectral acceleration at 0.3 sec period. In these figures, the geographic divisions of Alameda County are “census tracts”, the geographical units considered in the HAZUS-MH calculations. In Figures A1 – A4, direct economic loss is shown as a loss density (\$Million / km²).

Annual loss exceedance curves for the WG02 source model and for variants thereof

Here we briefly examine loss exceedance curves for the WG02 source model and for several variations upon that model. The variations are designed to provide insight into the sensitivity of the loss calculations to assumptions (which are selectively relaxed) and epistemic uncertainty (which is hypothetically reduced) in the WG02 model.

Annual loss calculated for the WG02 source model

Figure 6a shows an annual loss exceedance curve for the WG02 “official weights” model. The median annual economic loss in Alameda Co. is approximately \$140M. Figure 6b shows that in the WG02 model, the three largest contributing sources to the total annual loss in Alameda Co. are HS, HS+HN, and CN. Using a different set of source, attenuation and site models, Grossi (2000) found the average annual direct economic loss in Oakland, California, to be \$183M. But recall that only source model uncertainty is represented in our study. If uncertainty in the attenuation model, site conditions, building inventory, and building vulnerability were included as well, the right tail of the loss exceedance curve in Figure 6a would be greatly extended, as we saw in the analytical model. For example, the 1% “worst case” annual loss found by Grossi for Oakland, California, is \$3.1 billion. In contrast, in our study, the 1% loss (i.e., the ‘100-year loss’) is approximately \$200M. We believe that the discrepancy is due largely to the fact that our study omits uncertainty in attenuation, site, and building inventory and vulnerability models.

Dependence of loss exceedance curve on the choice of M-logA relation

Figure 7 shows loss exceedance curves for the WG02 source model, giving full weight, in turn, to each of the five M-logA relations considered by WG02, and for the officially weighted model. These loss distributions are approximately normal, with approximately equal variance, but with widely differing medians.

Dependence of loss exceedance curve on uncertainty in fault slip rate and segmentation.

Figure 8 shows the annual loss exceedance curves for variations upon the WG02 model in which epistemic uncertainty in slip rate, segment endpoint location, and both slip rate and segment location is removed. The uncertainty in slip rate and segmentation endpoint locations are symmetrical in the WG02 model, and, not surprisingly, the loss distribution is insensitive to these variations.

Deaggregation of loss over the seven major faults in the SFBR.

Figure 9 shows loss exceedance curves for earthquake sources on all faults in the SFBR, and on three subsets of these faults. The background sources are included in all of these curves. The figure shows that about half the annual loss in Alameda Co. is associated with the Hayward-Rodgers Creek fault, and approximately 90% of the loss arises from the San Andreas, Hayward-Rodgers Creek and Calaveras faults (and the background).

Deaggregation of loss with respect to the magnitude ranges of rupture sources.

Figure 10 shows the contribution to the loss exceedance curves as a function of the magnitude range of earthquakes. In the WG02 model, rupture sources with $6.7 \leq M < 7.0$ contribute approximately half the loss and earthquakes with $M \geq 7.5$ contribute about 15% of the loss in Alameda Co., on average.

High and low slip rates on faults.

Figure 11 shows the dependence of the loss on slip rate. WG02 represented the slip rate on each fault with symmetrical three-point and five-point distributions. Alternately using only the highest and only the lowest slip rates in these distributions increases and decreases, respectively, the loss (not surprisingly). WG02 also applied regional constraints to the total slip across the region to assure that the regional model remains consistent with the contemporary plate motion. Widening the regional constraint to 31-48 mm/yr (in addition to alternately using only the highest and lowest slip rates) further increases and decreases the loss (also not surprisingly). Narrowing the regional slip rate constraint (to 38-41 mm/yr) diminished the effect of low slip rates on faults by eliminating combinations of fault slip rates that exceed the lower bound of the regional constraint. The corresponding result for narrowed regional slip rate constraint and high fault slip rates is not shown; these constraints did not allow sufficient viable models. Figure 12 shows that merely widening the regional slip rate constraint (without altering the distributions of slip rate on the individual faults) does nothing to the loss distribution.

Aseismic slip on faults

WG02 allowed for the occurrence of aseismic slip (creep) on each fault in the model by specifying an aseismic slip factor (ASF). The faults with significant amounts of aseismic slip in the WG02 model are the Hayward, Calaveras and

Concord-Green Valley faults. Figure 13 shows that increasing or decreasing the assumed values of ASF does not affect the total loss, but does affect the relative contributions to the loss from larger and smaller magnitude events in the region. With more creep (lower ASF), small earthquakes account for an increased share of the loss: 50% of the loss is contributed by $M < 6.7$ earthquakes (Figure 13a). With less creep (higher ASF), the relative contribution from small earthquakes is diminished: only 20% of the loss is from $M < 6.7$ events (Figure 13b).

Probability models

Figure 14 shows the distribution of annual loss in Alameda Co. associated with each of the four probability models considered by WG02 for the SF Bay region. The median annual loss in the WG02 “official” model is \$162M. The ranking of median annual loss estimated for these models is the same as the ranking of probability of $M \geq 6.7$ earthquakes on the Hayward/Rodgers Creek fault (see WG02, Figure 6.8, top-right panel), owing to the fact that this fault accounts for approximately half of Alameda County’s risk (Figure 6b). Relative to the WG02 model, the BPT and BPT-step models yield higher annual loss (median values of \$224M and \$204M, respectively) and the Poisson and Empirical, lower (median values of \$134M and \$77M, respectively).

The greatest contrast between these distributions is in their right tails. The “worst-case” (1% exceedance) annual loss is \$483M and \$462M for the BPT and BPT-step probability models, respectively, \$436M for the WG02 weighted model, and \$181M and \$114M for the Poisson and Empirical models, respectively. The contrast between the time-dependent and time-independent probability models arises from two sources: the uncertainty associated with the date of last event and aperiodicity in recurrence (neither of which is used in the Poisson model); and, in the case of the WG02 weighted model, the averaging of multiple probability models, which introduces additional epistemic uncertainty in the form of diversity in expert opinion. Necessarily, the worst-case loss in the averaged model is close in value to the worst-case loss in the individual model with the highest worst-case loss. In terms of the annual economic loss estimate for Alameda Co., WG02’s decision to employ a suite of time-dependent probability models rather than use only the long-term time-independent probability model increased the median annual loss by only 20% but more than doubled the worst-case (1% exceedance) loss.

Figure 15 is a variation upon Figure 14 in which an additional loss exceedance curve is shown. The additional curve corresponds to the BPT_Step model in which the Hayward/Rodgers Creek fault is “relaxed”. This was accomplished by setting the date of last earthquake on each of the three segments in HRC to be 1990. Comparing this model to the normal BPT-Step model illustrates the level of risk in Alameda County (2002-2031) arising from the Hayward Fault relative to the risk from the rest of the San Francisco Bay Region.

References Cited

- Boore, D.M., W.B. Joyner and T.E. Fumal, 1993. Estimation of response spectra and peak accelerations from western North American earthquakes: an interim report, U.S. Geological survey Open-File Report 93-509.
- Boore, D.M., W.B. Joyner and T.E. Fumal, 1994. Estimation of response spectra and peak accelerations from western North American earthquakes: an interim report Part 2, U.S. Geological survey Open-File Report 94-127.
- Borcherdt, R.D., 1994. Estimates of site-dependent response spectra for design (methodology and justification), *Earthquake Spectra* **10**, 617-653.
- Campbell, K.W. and Y. Bozorgenia, 1994. Near-source attenuation of peak acceleration from worldwide accelerograms recorded from 1957 to 1993, in Proceedings of Fifth U.S. National Conference on Earthquake Engineering, Earthquake Engineering Research Institute **3**, p. 283-393.
- Cao, T., and M.D. Petersen, Uncertainty of earthquake losses due to model uncertainty of input ground motions in the Los Angeles Area, *Bull. Seismo. Soc. Amer.*, in press.
- Cao, T., M.D. Petersen, C.H. Cramer, T.R. Toppozada, M.S. Reichle, and J.F. Davis, 1999. The calculation of expected loss using probabilistic seismic hazard, *Bull. Seismo. Soc. Amer.*, **89**.
- Field, E.H., T.H. Jordan, C.A. Cornell, 2003. OpenSHA: A developing community-modeling environment for seismic hazard analysis, *Seism. Res. Lett.* **74**, Number 4, 406-419.
- Field, E.H., N. Gupta, V. Gupta, M. Blanpied, P. Maechling, and T.H. Jordan, 2005a. Hazard calculations for the WGCEP-2002 earthquake-rupture forecast using OpenSHA and distributed object technologies, *Seism. Res. Lett.* **76**, 161-167.
- Field, E.H., H.A. Seligson, N. Gupta, V. Gupta, T.H. Jordan, and K.W. Campbell, 2005b. Loss estimates for a Puente Hills blind-thrust earthquake in Los Angeles, California, *Earthquake Spectra* **21**, 329-338.
- Frankel, A.D., M.D. Petersen, C.S. Mueller, K.M. Haller, R.W. Wheeler, E.V. Leyendecker, R.L. Wesson, S.C. Harmsen, C.H. Cramer, D.M. Perkins, and K.S. Rukstales, 2002. Documentation for the 2002 update of the National seismic hazard maps, *USGS Open-File Report* 02-420.
- Grossi, P., 2000. Quantifying the uncertainty in seismic risk and loss estimation, Ph.D. Thesis, University of Pennsylvania, Dept. of Systems Engineering.
- HAZUS-MH Technical Manual, 2003. Federal Emergency Management Agency (FEMA), <http://www.fema.gov/hazus>.
- Sadigh, K., C.Y. Chang, N.A. Abrahamson, S.J. Chiou and M.S. Power, 1993. Specification of long-period ground motions: updated attenuation relationships for rock site conditions and adjustment factors for near-field effects, in Proceedings of ATC-17-1 Seminar on Seismic Isolation, Passive energy Dissipation, and Active Control, Applied Technology Council, Redwood City.
- Wald, D.J., V. Quitoriano, T.H. Heaton, H. Kanamori, 1999. Relationships between peak ground acceleration, peak ground velocity and modified Mercalli intensity in California, *Earthquake Spectra*, **15**, 557-564.
- Wells, D.J. and K.J. Coppersmith, 1994. New empirical relationships among magnitude, rupture length, rupture width, rupture area and surface displacement, *Bull. Seism. Soc. Am.*, **84**, 974-1002.
- Working Group on California Earthquake Probabilities (WGCEP), 2003. Earthquake probabilities in the San Francisco Bay region: 2002-2031, *USGS Open-File Report* **03-214**.

Figures

Figure 1. Empirical ground motion, intensity and damage relationships. (a) Open circles show empirical relationship between peak ground acceleration (PGA) and modified Mercalli intensity (MMI) (see Table 1), taken from Wald et al. (1999) and used in ShakeMap. Solid line is an analytical function designed to approximate the Wald et al. (1999) points and defined in the text in Equation 2a. (b) Open circles show empirical relationship between MMI and Central Damage Factor (see Table 2) determined by ATC-13. Damage factor is defined in ATC-13 as the dollar loss divided by the replacement value. Central damage factor (CDF) is the mean of a distribution of damage factors for wood-frame low-rise buildings, for a given shaking intensity (MMI), determined by ATC-13 (Table 7.10) based on expert opinion. Solid line is an analytical function designed to approximate the CDF points in ATC-13 and defined in the text in Equation 2b.

Figure 2. Three arbitrary, truncated Gaussian distributions representing distributions of PGA. Mean PGA (before truncation) for all three distributions is 0.5 g. Standard deviations are 0.05, 0.2 and 0.4 g.

Figure 3. Distributions of MMI corresponding to the distributions of PGA in Figure 2 and the empirical relation between PGA and MMI of Wald et al. (1999) and shown in Figure 1a. Increasing width in distribution of PGA produces increasing widths in distribution of MMI and progressive shifting of median MMI to the right (greater MMI).

Figure 4. Distributions of Central Damage Factor (CDF) (see text) corresponding to the distributions of MMI in Figure 3 and the empirical relation between MMI and CDF shown in Figure 1b. Solid lines indicate distributions of CDF. Median CDF values shift slightly to the right. The 95%-ile values of CDF (indicated by vertical dashed lines) shift dramatically upward with increasing width of PGA and MMI distributions.

Figure 5. Probability of exceedance curves for the three distributions of CDF shown in Figure 4.

Figure 6. (a) Annual loss exceedance curve for Alameda County, California, calculated with Hazus-MH and corresponding to the WG02 source model for the San Francisco Bay Region. (b) Pie chart showing relative contributions to the annual loss in (a) of the ten rupture sources in the WG02 model contributing the greatest loss. Key: “hs”=southern Hayward fault; “hs+hn”=full Hayward fault; “cn”=northern Calaveras fault; “sas+sap+san+sao”=full San Andreas fault; “hn”=northern Hayward fault; “mtd”=Mt. Diablo fault; “hs+hn+rc”=Hayward and Rodgers Creek fault; “hn+rc”=northern Hayward and Rodgers Creek faults”, “cs+cc+cn”=full Calaveras fault; “sas+sap”=Santa Cruz and Peninsula segments of San Andreas fault.

Figure 7. Variations upon the loss exceedance curve for Alameda County shown in Fig 6a, corresponding to alternative relationships between rupture area and magnitude (M-logA relationships). The WG02 model used a weighted average of five M-logA relationships (heavy solid line). Other lines are loss exceedance curves for source models using individual M-logA relationships (100% weighting). Abbreviations correspond to those used in WG02 (2003): E1 and E2 correspond to their Equations 4.5a and 4.5b; H1 and H2 correspond to their Equations 4.6a and 4.6b; W&C corresponds to the Wells and Coppersmith (1994) relationship.

Figure 8. Annual loss exceedance curves for Alameda County for variations upon the WG02 (2003) model in which the epistemic uncertainty in slip rate (“Slip”), segment endpoint location (“Geom”), and both slip rate and segment location is removed.

Figure 9. Annual loss exceedance curves for Alameda County for earthquake sources on all faults in the SFBR (heavy line) and on three subsets of these faults. The background source is included in all of these curves. SAF=San Andreas fault; HRC=Hayward/Rodgers Creek fault; CLV=Calaveras fault.

Figure 10. Annual loss exceedance curves for Alameda County for all earthquake sources in the SFBR (heavy line) and for four subsets of sources with descending maximum magnitude.

Figure 11 Annual loss exceedance curves for Alameda County corresponding to the WG02 (2003) model (heavy line) and for variations upon this model in which slip rates are alternately skewed up (“High slip rates”) and down (“Low slip rates”) relative to the slip rate distribution assumed in the WG02 model, and also allowed to vary more widely (“wide regional constraint”). The WG02 model constrains sums of slip rate on fault segments in three transverse cross-sections in the Bay region with the geodetically-determined range 36—43 mm/yr. The “wide regional constraint” curves widen this constraint to 31—48 mm/yr. The “narrow regional constraint” curve corresponds to the range 38—41 mm/yr.

Figure 12. Annual loss exceedance curves for Alameda County corresponding to the WG02 (2003) model (solid line) and for a variation upon this model (dashed line) in which the regional slip rate constraint is widened to 31—48 mm/yr, but the slip distribution of slip rate on each fault is unchanged relative to the WG02 model.

Figure 13. Annual loss exceedance curves for Alameda County corresponding to variations upon the WG02 (2003) model in which the distribution of aseismic slip is altered. **(a)** Distribution of aseismic slip on the faults is skewed up (all weight on the lowest value of the “ASF” parameter in the WG02 model; faults are more creeping). Curves correspond to varying maximum magnitude of earthquakes used in the loss calculation. **(b)** Distribution of aseismic slip on the faults is skewed down (all weight on the highest value of “ASF” parameter in the WG02 model; faults are more locked).

Figure 14. Annual loss exceedance curves for Alameda County corresponding to the WG02 (2003) model (heavy line) and for variations upon this model in which each of the individual probability models in the WG02 model is used with full weight. Numbers shown after each model name in legend are the median annual loss and “worst-case” (1% exceedance) loss, both in \$Million.

Figure 15. Annual loss exceedance curves for Alameda County as in Figure 14, with an additional loss exceedance curve is shown. The additional curve corresponds to the BPT_Step model in which the Hayward/Rodgers Creek fault is “relaxed”. This was accomplished by setting the date of last earthquake on each of the three segments in HRC to be 1990.

Figure A1. Ground motions and direct economic loss caused by rupture of the Southern Hayward fault (segment HS, magnitude 6.7). This scenario is, on average, considering its impact and mean recurrence interval, the largest contributor to the expected losses for Alameda County. Ground motions (contours) are pseudo-acceleration spectra (g) at 0.3 sec period on hard rock sites, calculated with OpenSHA ShakeMap software. Direct economic loss, shown for each census tract in Alameda Co., includes losses coming from building damage, contents damage, inventory loss, relocation costs, income loss, rental income loss and wages loss. It does *not* include losses due to interruption of business, increased social services, reduced tax revenues, and losses associated with injuries, fatalities and other human loss that also would result from a major quake. The expected total direct economic loss in Alameda Co. for this earthquake scenario is \$8.9 billion.

Figure A2. Ground motions and direct economic loss caused by rupture of the entire Hayward fault (segments HS+HN, magnitude 6.9). This scenario is, on average, the second largest contributor to the expected losses for Alameda County. Ground motion (contours) and economic loss are as in Figure A1. The expected total direct economic loss in Alameda Co. for this earthquake scenario is \$11.0 billion.

Figure A3. Ground motions and direct economic loss caused by rupture of the northern segment of the Calaveras fault (segment CN, magnitude 6.8). This scenario is, on average, the third largest contributor to the expected losses for Alameda County. Ground motion (contours) and economic loss are as in Figure A1. The expected total direct economic loss in Alameda Co. for this earthquake scenario is \$3.8 billion.

Figure A4. Ground motions and direct economic loss caused by rupture of the entire San Andreas fault (segments SAS+SAP+SAN+SAO, magnitude 7.9). This scenario is, on average, the fourth largest contributor to the expected losses for Alameda County. Ground motion (contours) and economic loss are as in Figure A1. The expected total direct economic loss in Alameda Co. for this earthquake scenario is \$4.6 billion.

Figure 1a

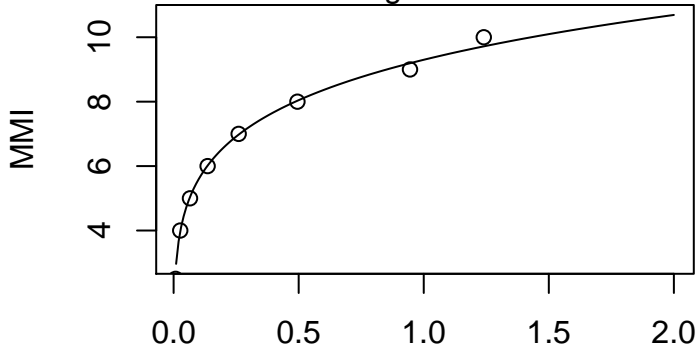


Figure 1b

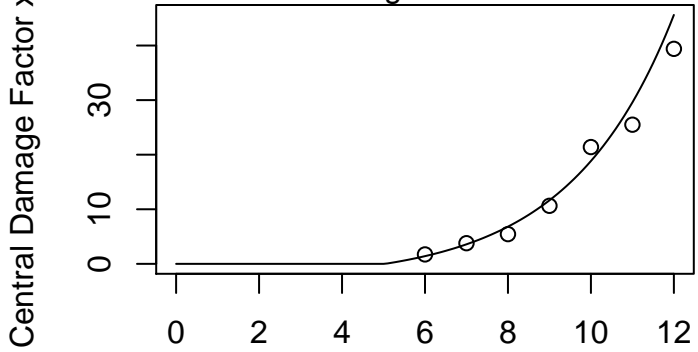


Figure 2

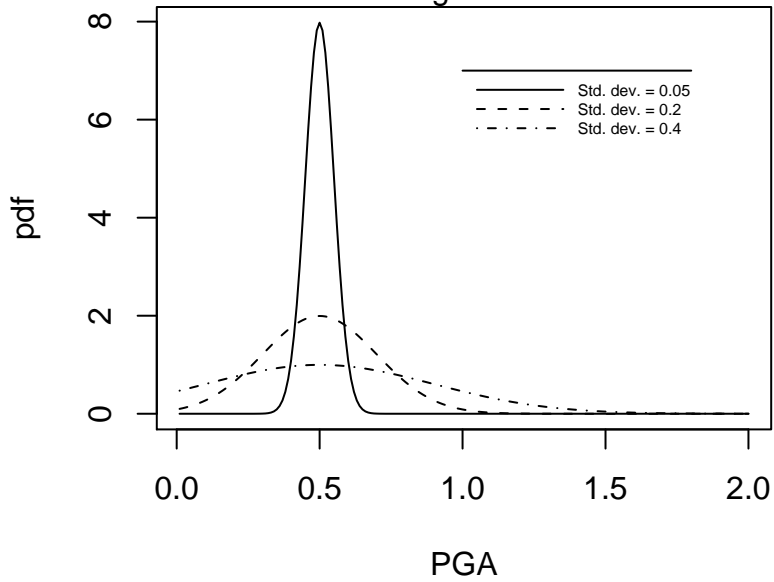


Figure 3

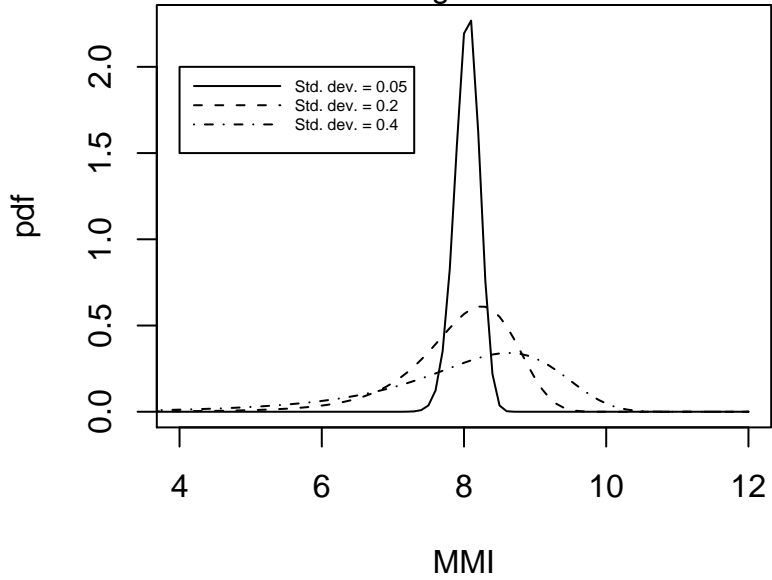


Figure 4

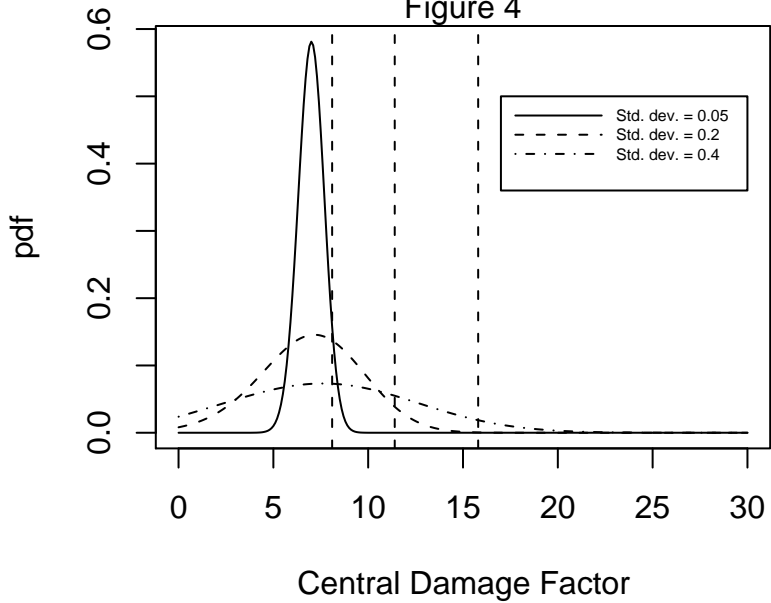


Figure 5

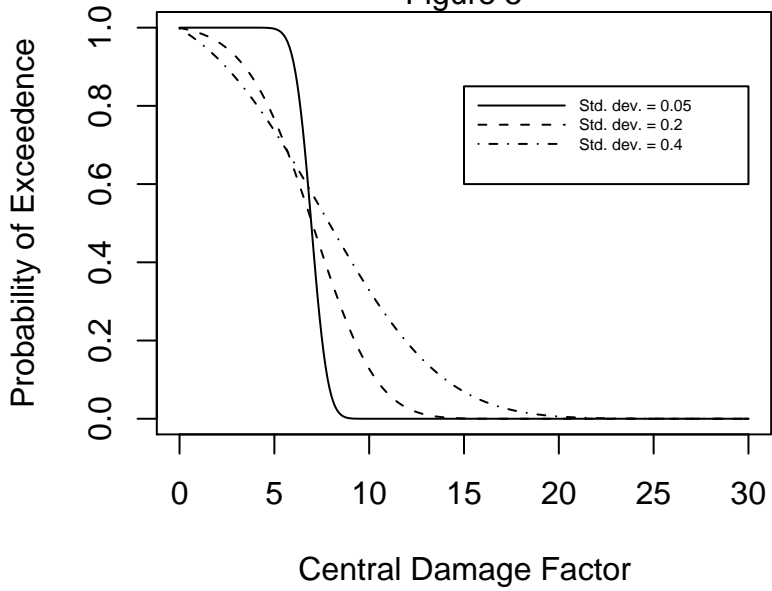
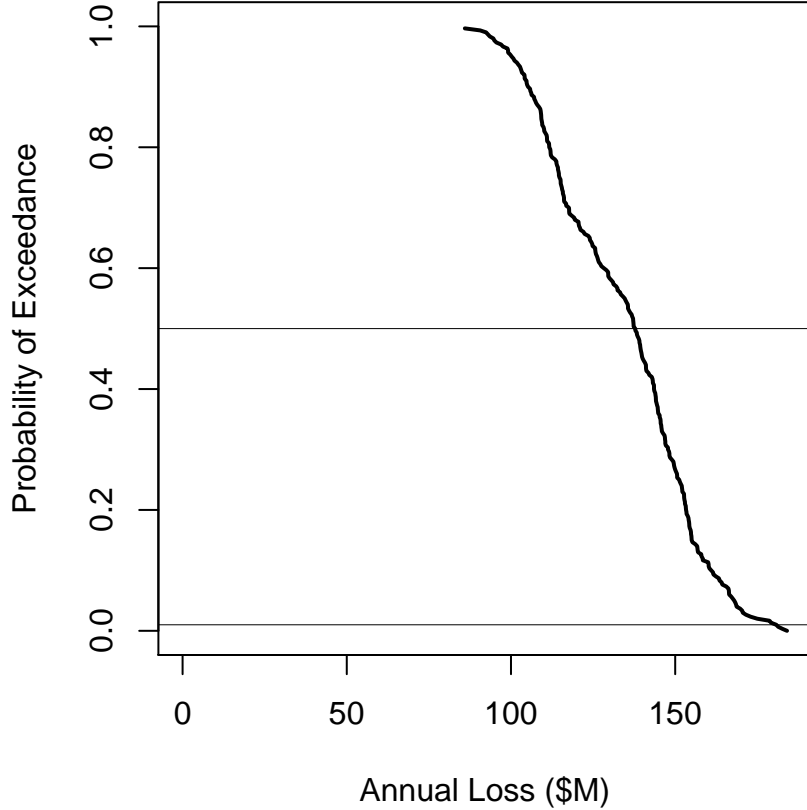


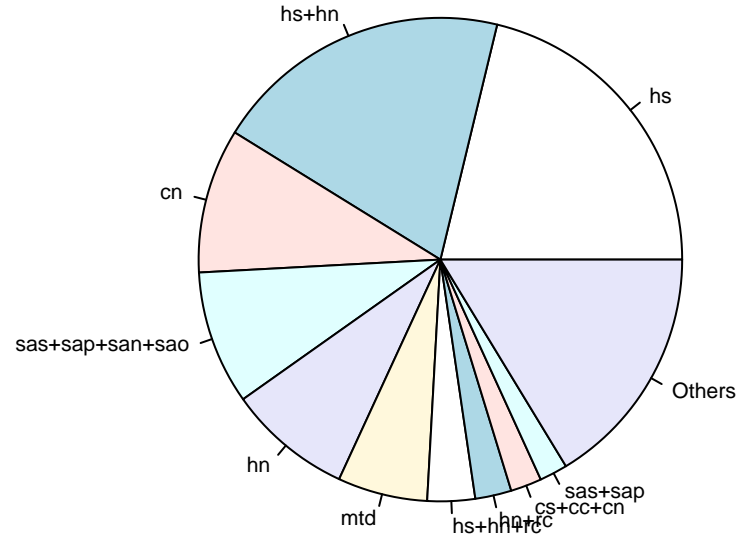
Figure 6

Direct Economic Loss

Alameda County

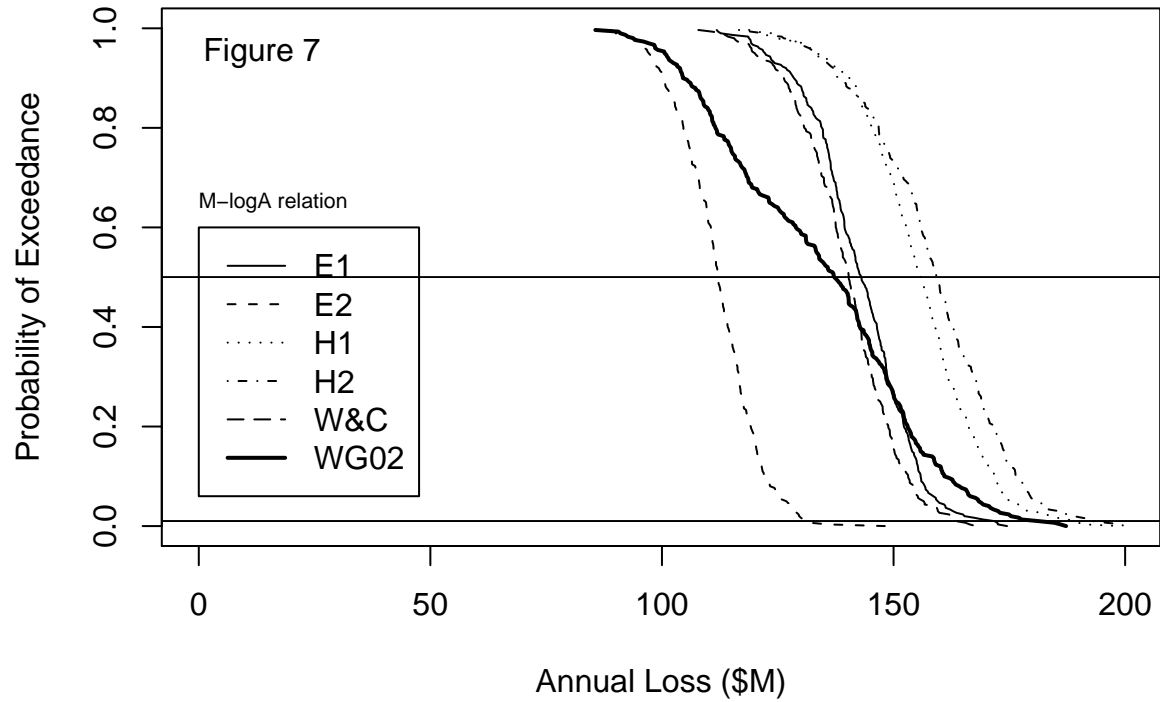


Top 10 Contributors



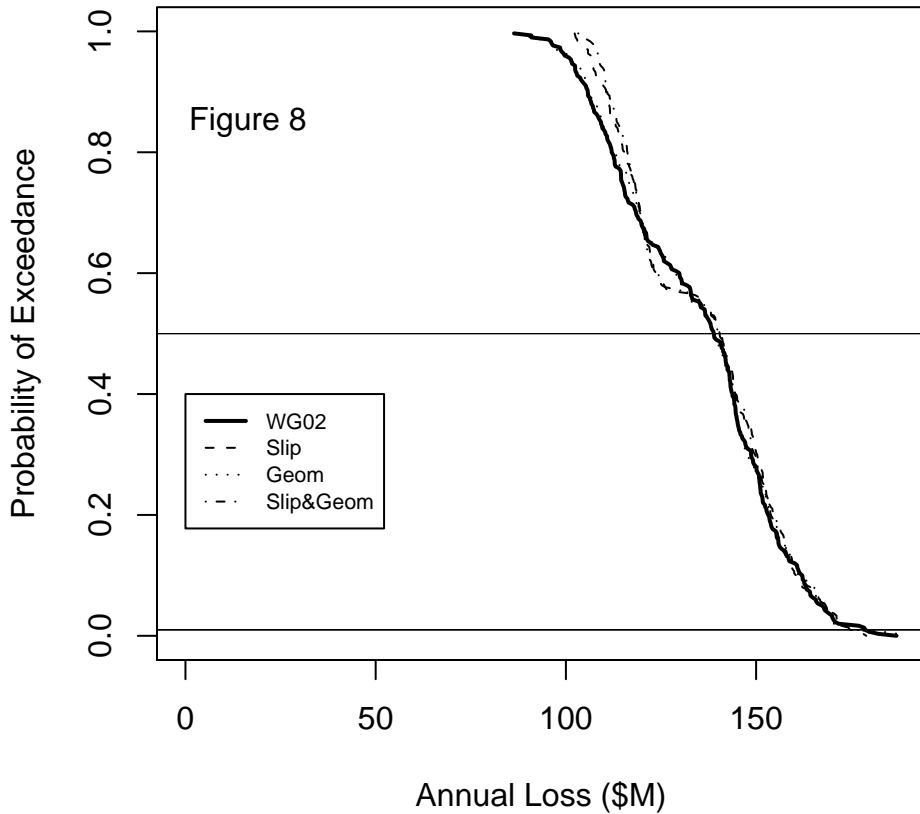
Direct Economic Loss

Alameda County



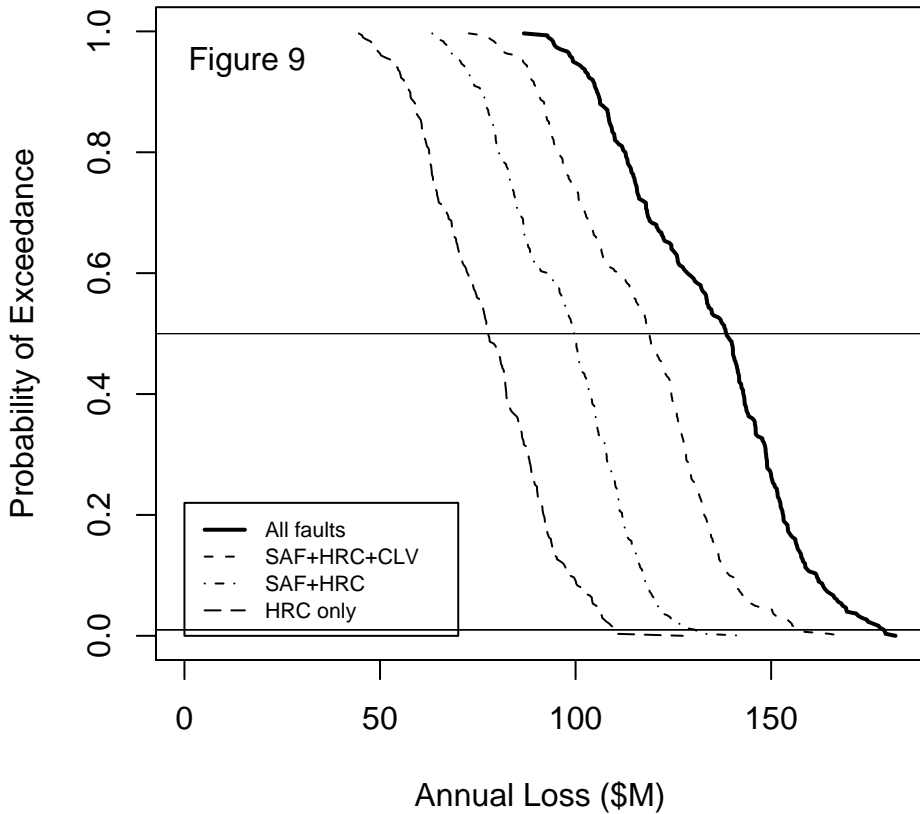
Direct Economic Loss

Alameda County



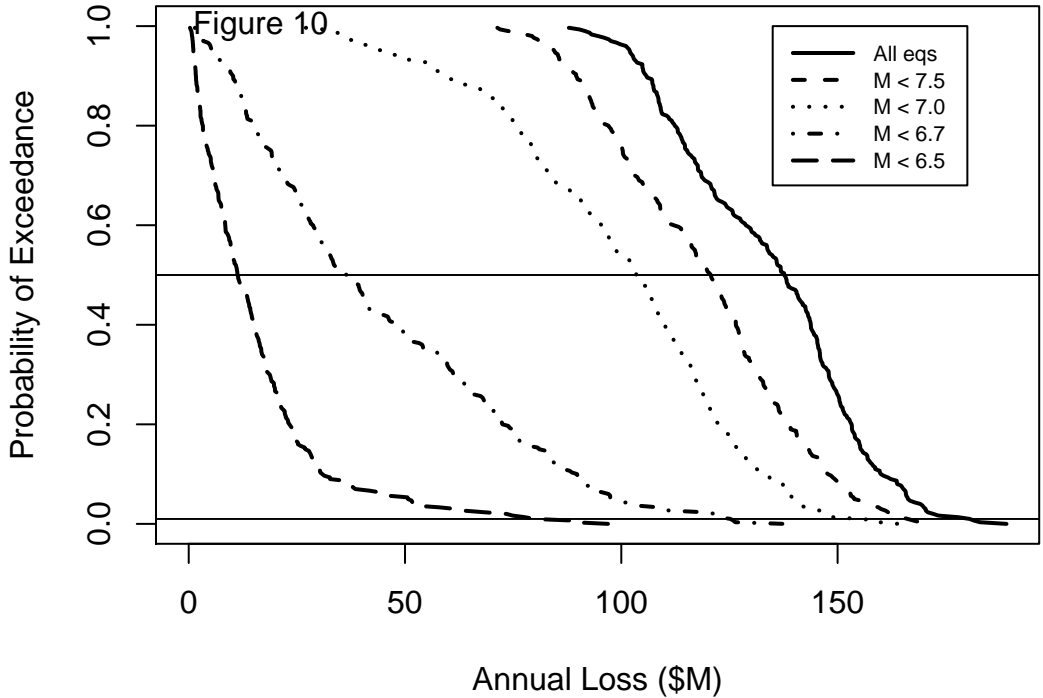
Direct Economic Loss

Alameda County



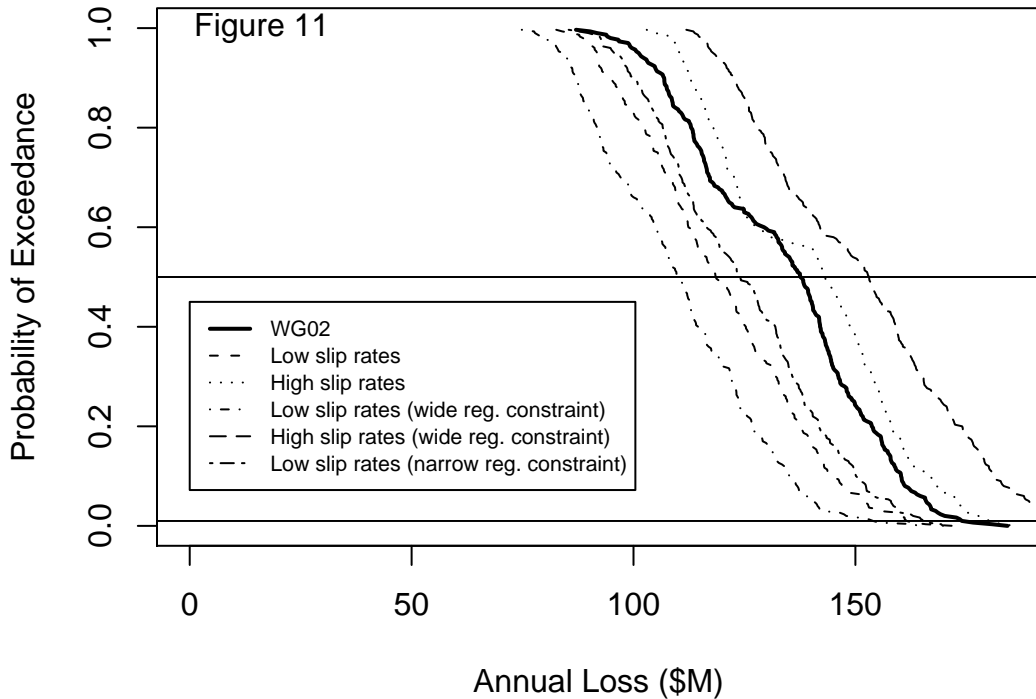
Direct Economic Loss

Alameda County



Direct Economic Loss

Alameda County



Direct Economic Loss

Alameda County

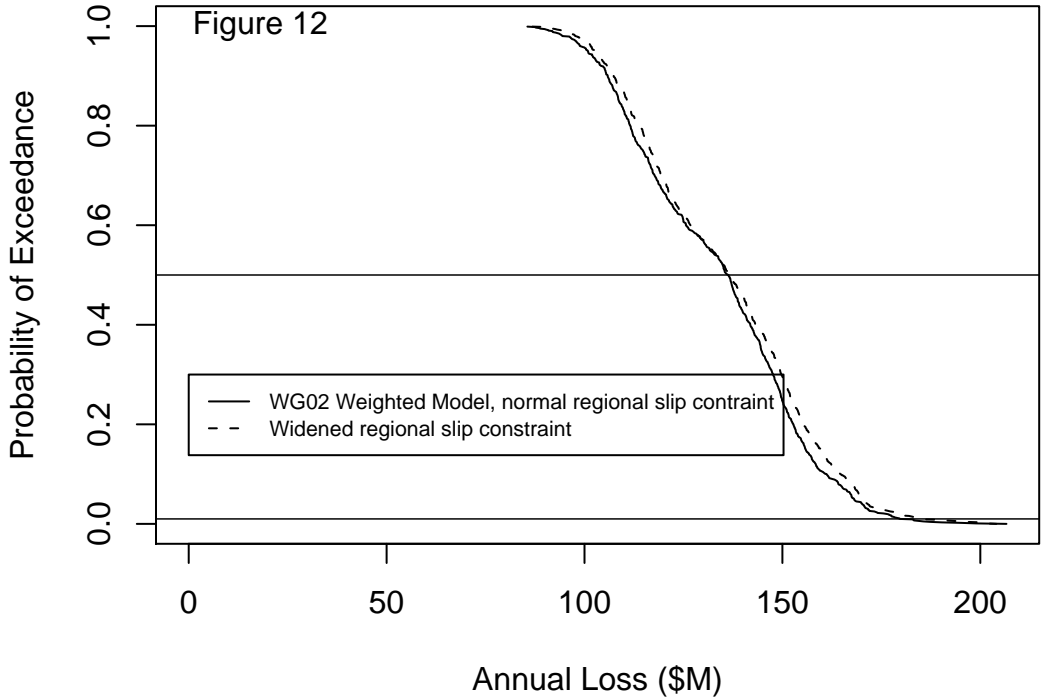


Figure 13a

Direct Economic Loss
Alameda County

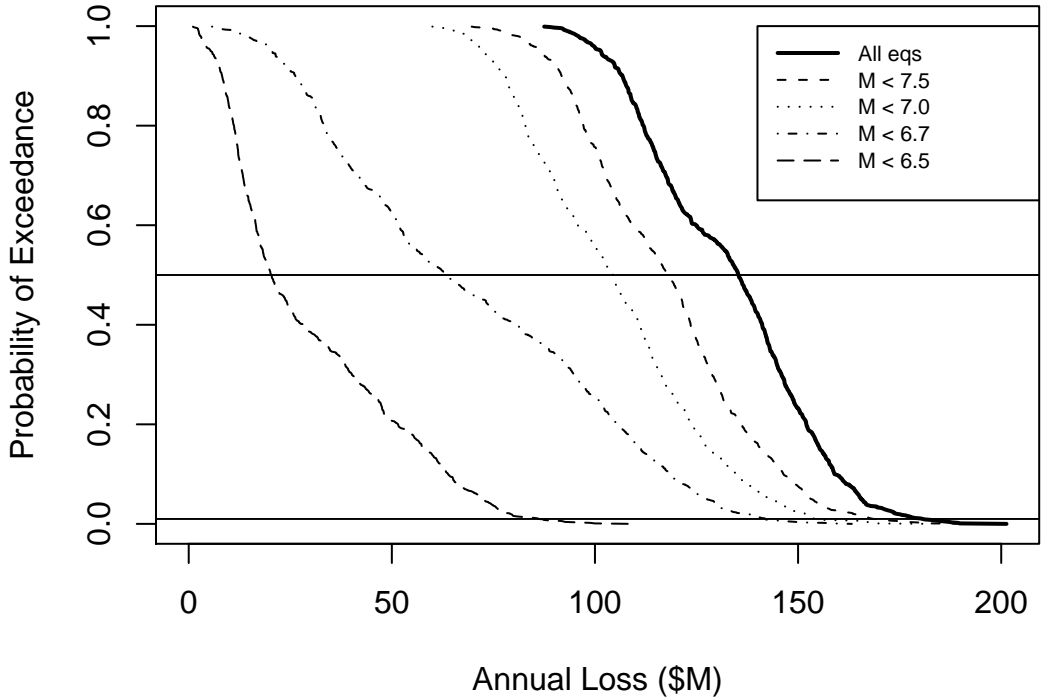


Figure 13b – High ASF

Direct Economic Loss

Alameda County

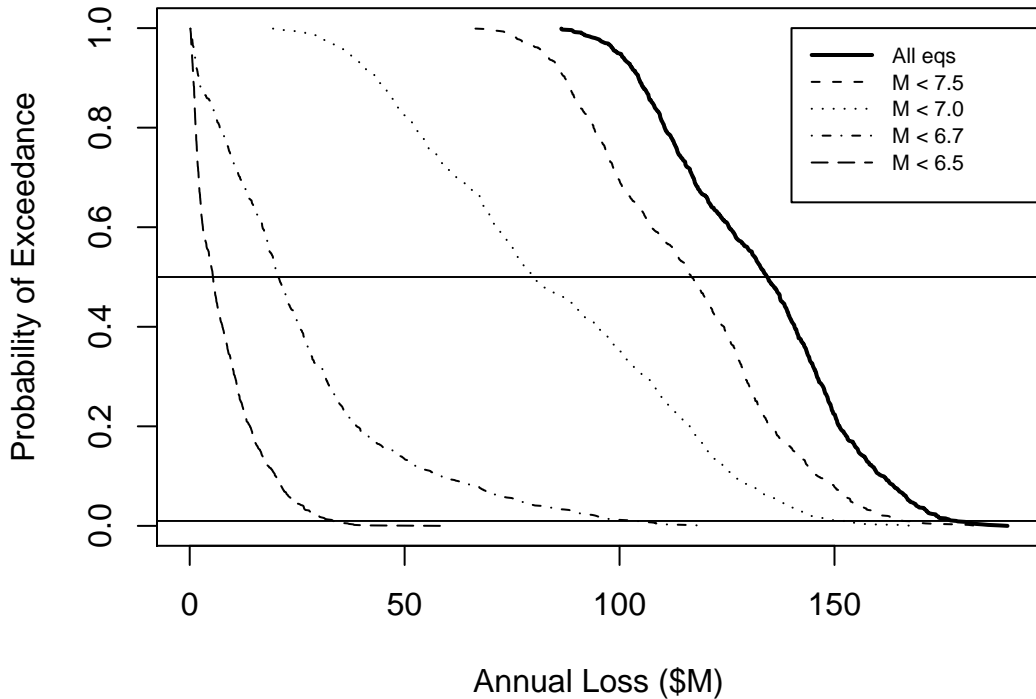
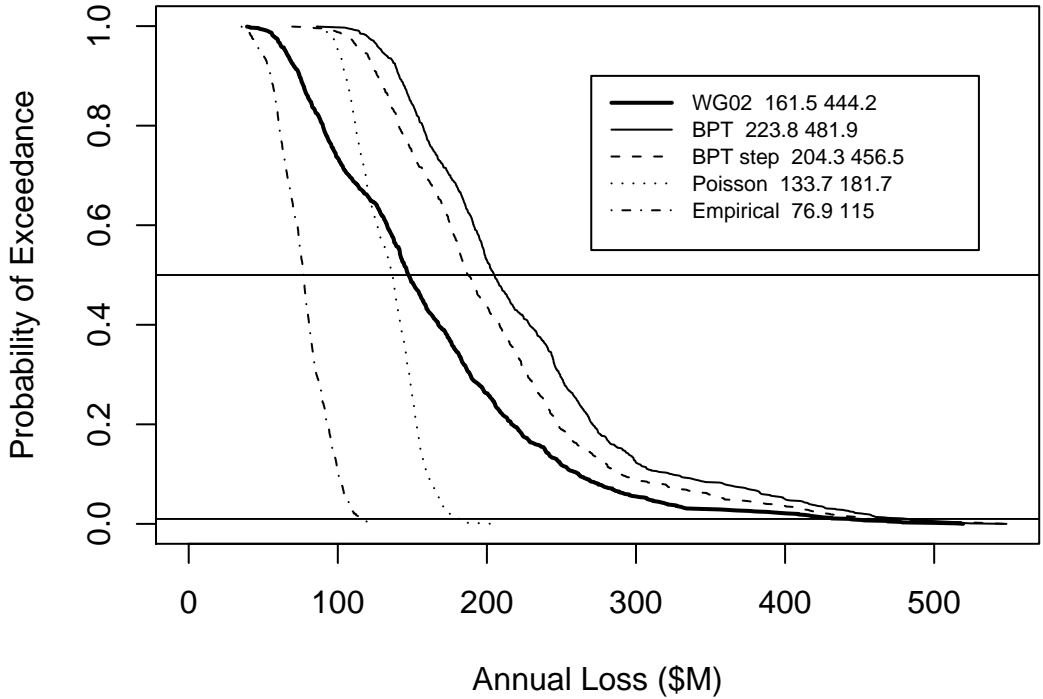


Figure 14

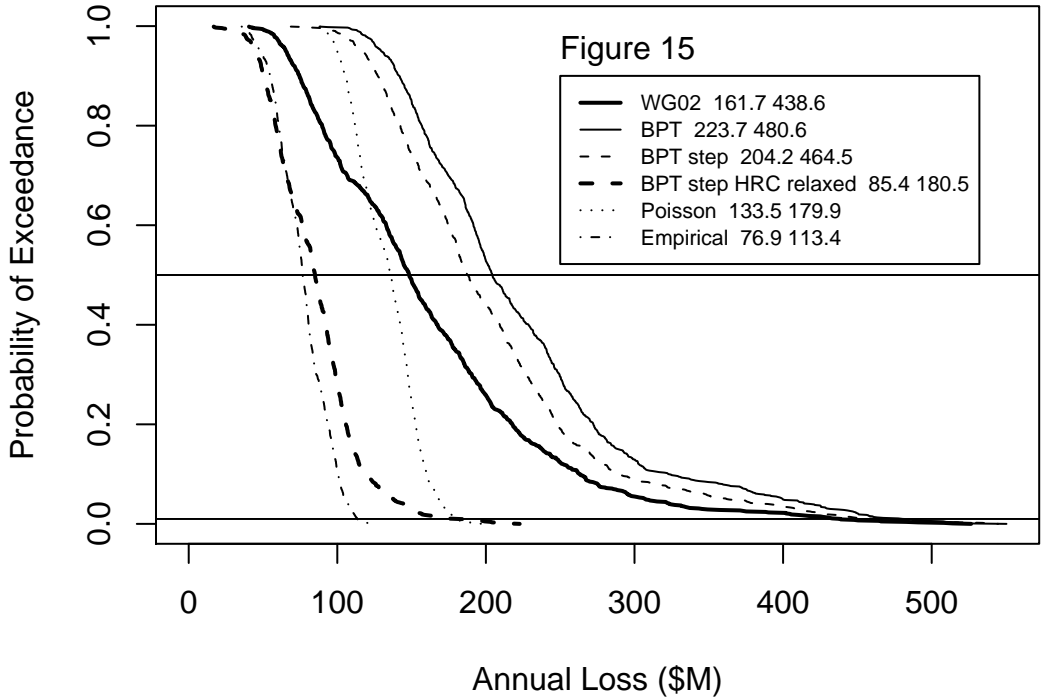
Direct Economic Loss

Alameda County



Direct Economic Loss

Alameda County



Earthquake Scenario: HS M=6.7

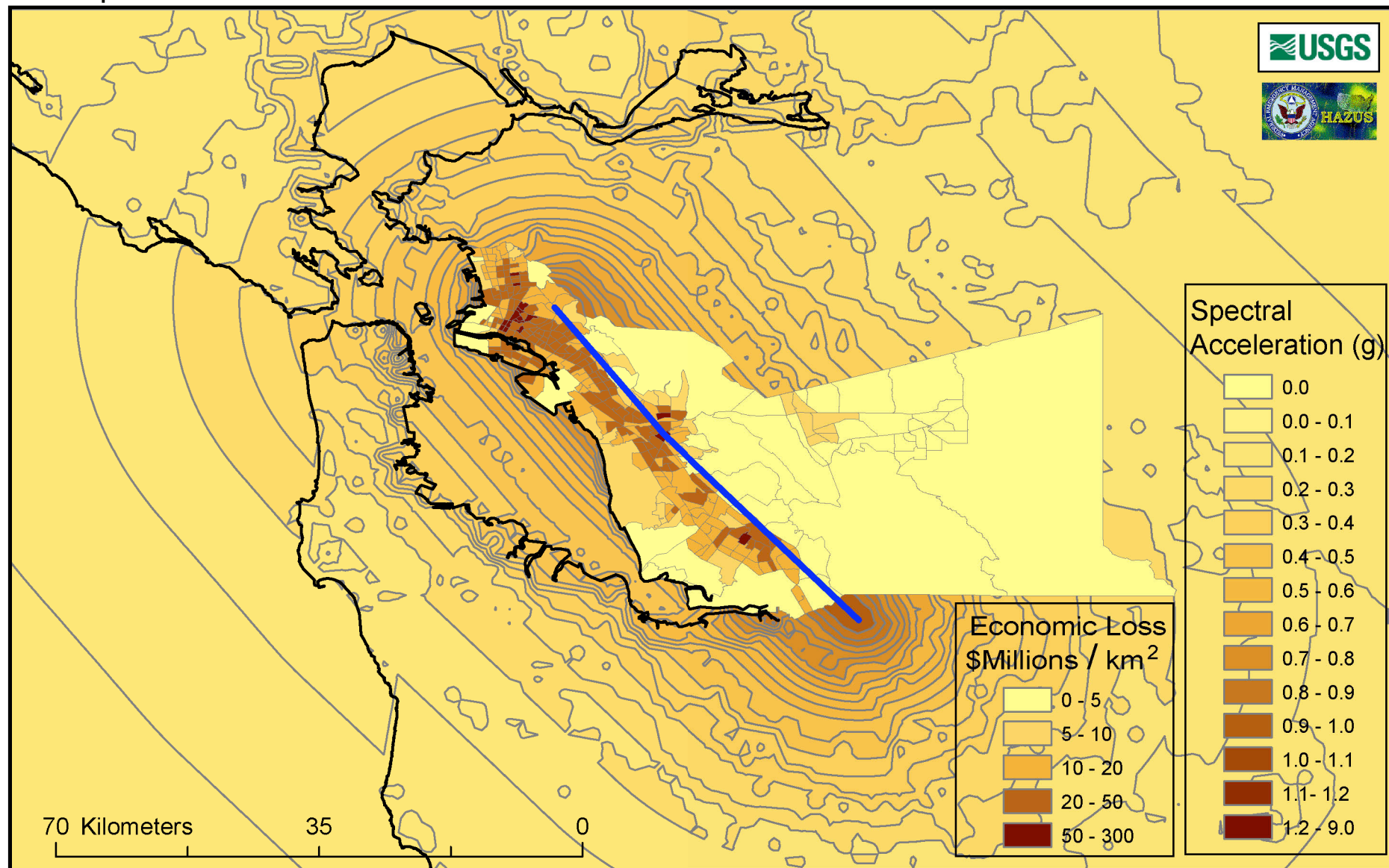


Figure A1. Ground motions and direct economic loss caused by rupture of the Southern Hayward fault (segment HS, magnitude 6.7, blue line). This scenario is, on average, considering its impact and mean recurrence interval, the largest contributor to the expected losses for Alameda County. Ground motions (contours) are pseudo-acceleration spectra (g) at 0.3 sec period on hard rock sites, calculated with OpenSHA ShakeMap software. Direct economic loss, shown for each census tract in Alameda Co., includes losses coming from building damage, contents damage, inventory loss, relocation costs, income loss, rental income loss and wages loss. It does not include losses due to interruption of business, increased social services, reduced tax revenues, and losses associated with injuries, fatalities and other human loss that also would result from a major quake. The expected total direct economic loss in Alameda Co. for this earthquake scenario is \$8.9 billion.

Earthquake Scenario: HS+HN M=6.9

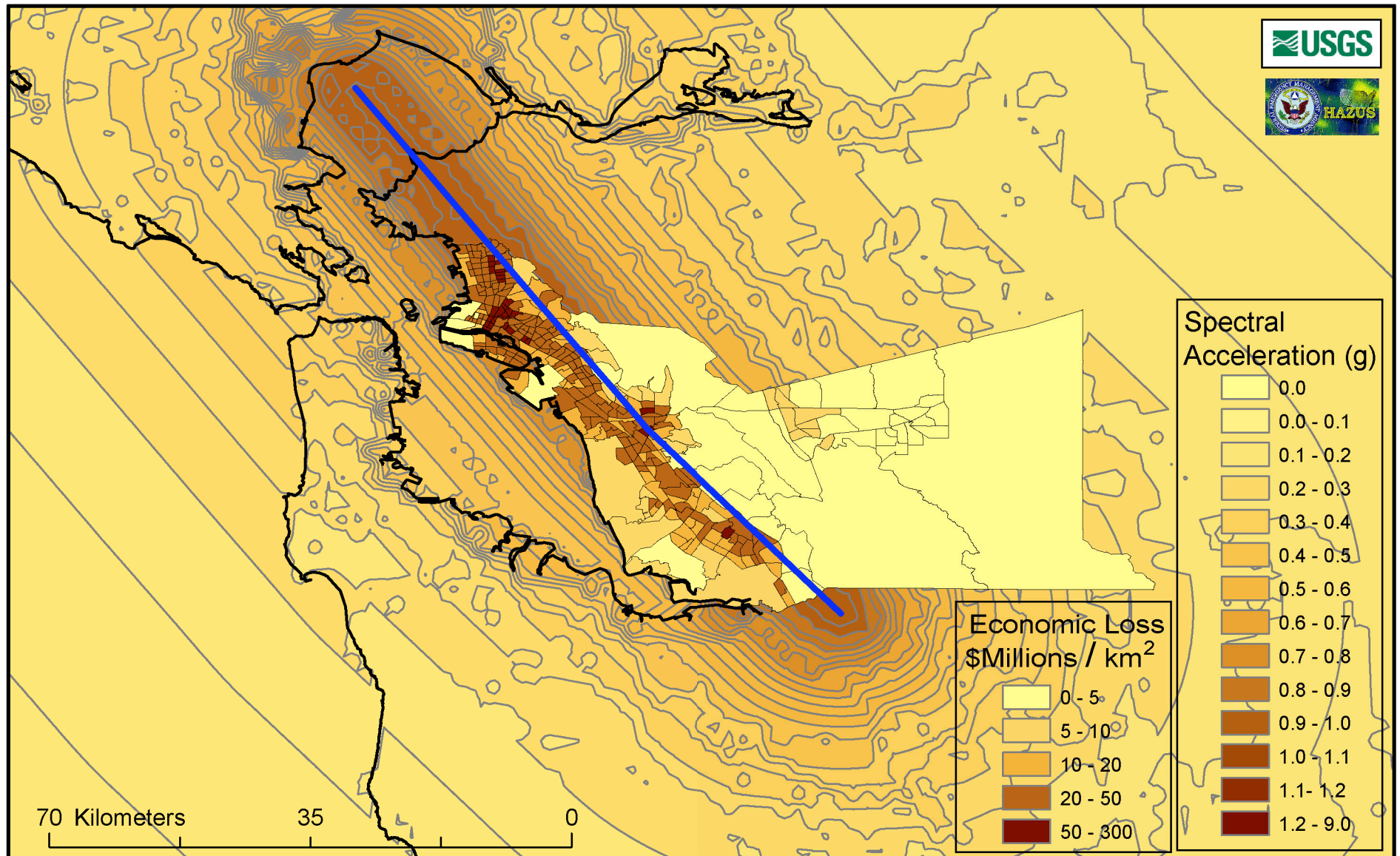


Figure A2. Ground motions and direct economic loss caused by rupture of the entire Hayward fault (segments HS+HN, magnitude 6.9, blue line). This scenario is, on average, the second largest contributor to the expected losses for Alameda County. Ground motion (contours) and economic loss are as in Figure A1. The expected total direct economic loss in Alameda Co. for this earthquake scenario is \$11.0 billion.

Earthquake Scenario: CN M=6.8

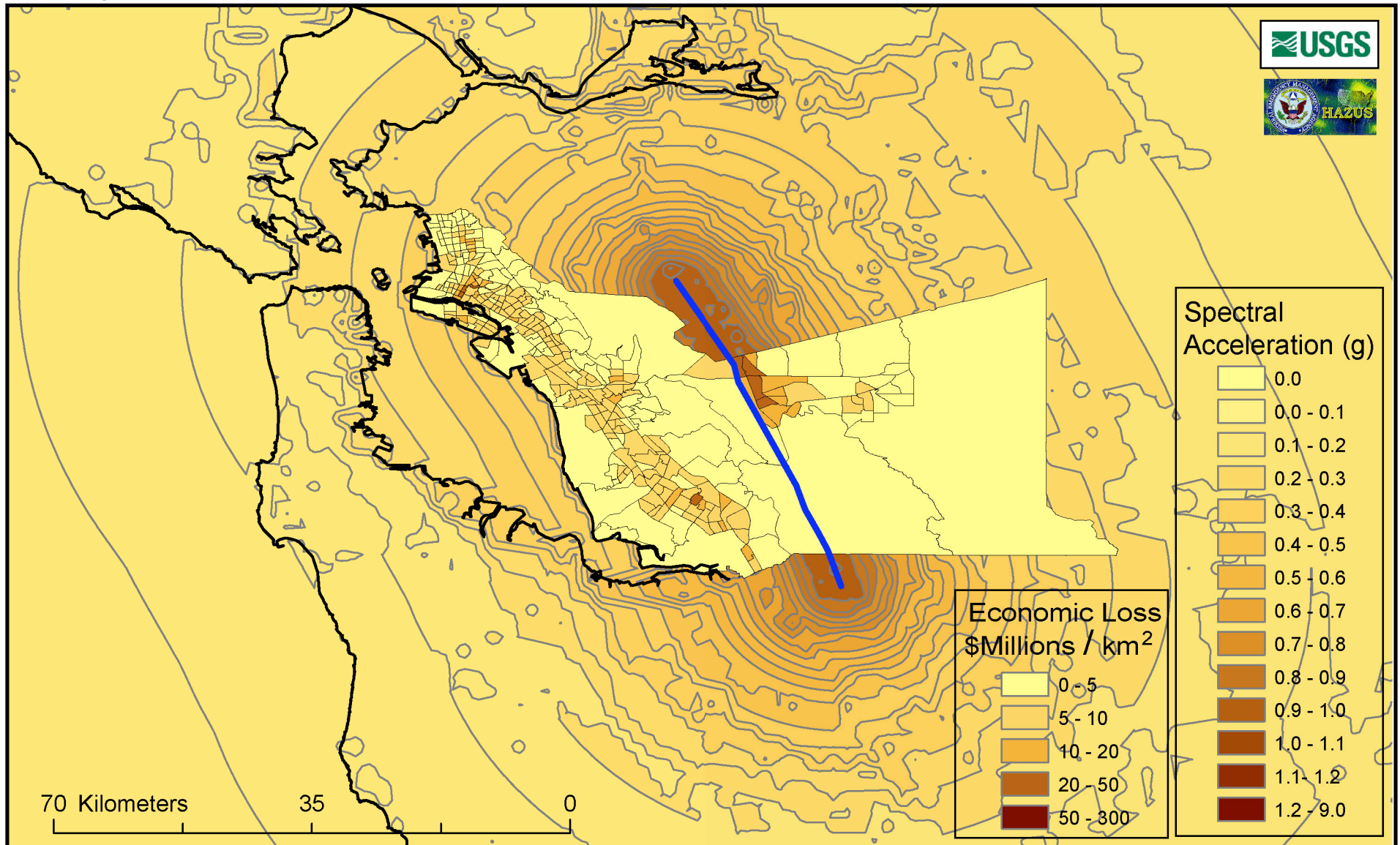


Figure A3. Ground motions and direct economic loss caused by rupture of the northern segment of the Calaveras fault (segment CN, magnitude 6.8, blue line). This scenario is, on average, the third largest contributor to the expected losses for Alameda County. Ground motion (contours) and economic loss are as in Figure A1. The expected total direct economic loss in Alameda Co. for this earthquake scenario is \$3.8 billion.

Earthquake Scenario: SAS+SAP+SAN+SAO M=7.9

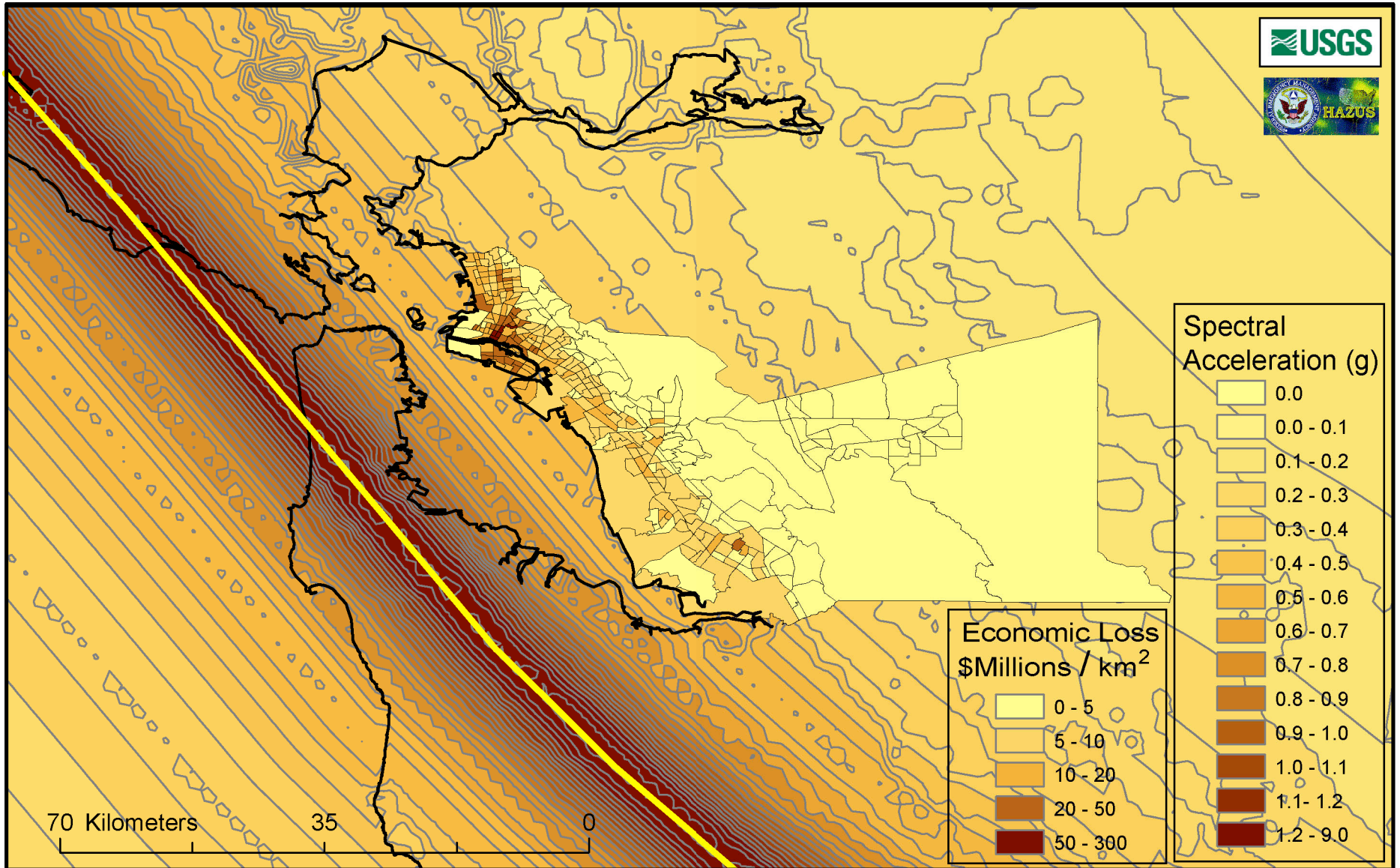


Figure A4. Ground motions and direct economic loss caused by rupture of the entire San Andreas fault (segments SAS+SAP+SAN+SAO, magnitude 7.9, yellow line). This scenario is, on average, the fourth largest contributor to the expected losses for Alameda County. Ground motion (contours) and economic loss are as in Figure A1. The expected total direct economic loss in Alameda Co. for this earthquake scenario is \$4.6 billion.